Solar-terrestrial coupling evidenced by periodic behavior in geomagnetic indexes and the infrared energy budget of the thermosphere

Martin G. Mlynczak[1]
F. Javier Martin-Torres[2]
Christopher J. Mertens[1]
B. Thomas Marshall[3]
R. Earl Thompson[3]
Janet U. Kozyra[4]
Ellis E. Remsberg[1]
Larry L. Gordley[3]
James M. Russell III[5]
Thomas Woods[6]

[1]NASA Langley Research Center, Hampton, VA
[2]Analytical Services and Materials, Inc., Hampton, VA
[3]G & A Technical Software, Newport News, VA
[4]University of Michigan, Ann Arbor, MI
[5]Hampton University, Hampton, VA
[6]Laboratory for Atmospheric and Space Physics, Boulder, CO

Abstract. We examine time series of the daily global power (W) radiated by carbon dioxide (at 15 μm) and by nitric oxide (at 5.3 μm) from the Earth's thermosphere between 100 km and 200 km altitude. Also examined is a time series of the daily absorbed solar ultraviolet power in the same altitude region in the wavelength span 0 to 175 nm. The infrared data are derived from the SABER instrument and the solar data are derived from the SEE instrument, both on the NASA TIMED satellite. The time series cover nearly 5 years from 2002 through 2006. The infrared and solar time series exhibit a decrease in radiated and absorbed power consistent with the declining phase of the current 11-year solar cycle. The infrared time series also exhibits high frequency variations that are not evident in the solar power time series. Spectral analysis shows a statistically significant 9-day periodicity in the infrared data but not in the solar data. A very strong 9-day periodicity is also found to exist in the time series of daily A_p and K_p geomagnetic indexes. These 9-day periodicities are linked to the recurrence of coronal holes on the Sun. These results demonstrate a direct coupling between the upper atmosphere of the Sun and the infrared energy budget of the thermosphere.

Introduction

The energy budget of the Earth's mesosphere and lower thermosphere remains a frontier of scientific inquiry. In order to obtain a basic scientific understanding of the terrestrial near-space environment and because of the potential for significant anthropogenic change in this region [e.g., *Roble and Dickinson*, 1989], NASA launched the Thermosphere-Ionosphere-Mesosphere Energetics and Dynamics (TIMED) satellite mission in December 2001. The

SABER experiment on TIMED is designed specifically to observe and quantify the energy budget through the measurement of key infrared emissions related to radiative cooling [*Mlynczak*, 1996; 1997]. The SEE instrument measures ultraviolet energy radiated by the Sun and relevant to the thermospheric energy balance [*Woods et al*., 2002]. The SABER and SEE data sets now exceed five years in length, offering a unique opportunity to study the climate and variability of the Earth's upper atmosphere. In this paper we present analyses of time series of radiated infrared power and absorbed solar power derived from TIMED measurements starting in January 2002 near solar maximum through December 2006 near solar minimum. These data demonstrate a strong coupling between the Sun, the Earth's geomagnetic environment, and the energy budget of the thermosphere. They are also the first long-term record of the main parameters that determine thermospheric climate, enabling fundamental tests against numerical models.

Methodology

We present calculations and analyses of the radiative energy in the atmosphere between 100 and 200 km altitude. Specifically we use the SABER data to compute the infrared radiated power (W) due to emission from nitric oxide (NO) at 5.3 μm and due to carbon dioxide (CO_2) at 15 μm. Similarly, we compute the absorbed power in the ultraviolet portion of the spectrum from 0 to 175 nm using data from the SEE instrument. The result of our calculations is the power radiated or absorbed, integrated over the entire Earth, for each individual day since the operational start of the TIMED mission in January 2002. The details of the calculation approach for NO are given in *Mlynczak et al*. [2005, 2007a]; for CO_2 in *Mlynczak et al*., [1999]; and for the solar ultraviolet power in *Mlynczak et al*., [2007b]. Briefly, the power radiated by CO_2 is obtained by vertically integrating the radiative cooling rates derived during the SABER

temperature retrieval process [*Mertens et al*., 2004] and available as a standard data product. At present we include only the fundamental ν_2 band of CO_2 which accounts for ~95% of the CO_2 emission. The power radiated by NO is obtained by vertical integration of the observed volume emission rate of energy followed by zonal and meridional integrations. In the case of solar power, we assume all radiation from 0 to 120 nm is absorbed, but we specifically compute the absorption in the 120 to 175 nm region. We choose 175 nm as a cut-off because it corresponds to the end of the Schumann-Runge continuum and because the atmosphere is essentially transparent above 100 km at longer wavelengths. The calculations presented here rely on versions 1.06 and 1.9 of the SABER and SEE data sets, respectively.

Results

Shown in Figure 1a are the time series of daily radiated power by CO_2 (blue curve) and NO from January 2002 through December 2006. In both CO_2 and NO two features are evident upon examination: substantial short-term (day-to-day) variations in the emitted power and a general decrease in the radiated power with time. In Figure 1b we show the time series of absorbed solar power (between 0 and 175 nm, blue curve) and the total (NO plus CO_2) infrared power. At present we have not included the infrared power from atomic oxygen at 63 μm as the TIMED satellite does not observe it. Clearly evident from visual inspection of Figure 1b is the long-term decrease in both the radiated and absorbed power. Also evident is substantial high-frequency variability in the infrared power that is not visually evident in the absorbed solar ultraviolet energy. There are in fact 10 days in which the emitted infrared power equals or exceeds the absorbed solar power. These results point to influences on the infrared energy budget other than from the absorption of solar ultraviolet photons.

Mlynczak et al. [2007b] began the examination of the variability of the NO time series (January 2002 through August 2006). They attributed the long-term decrease in NO emission to the decline of the current solar cycle. They also computed the Lomb Normalized Periodogram (LNP) of the NO time series and noted a statistically significant 9-day periodic feature, but did not discern its origin. Given the stark differences in appearance of the time series of absorbed solar power and emitted infrared power in Figure 1b, we continue this analysis by computing the LNP of the solar and infrared time series and also of the time series of the daily F10.7 solar index and the daily A_p and K_p geomagnetic indexes.

Shown in Figures 2a and 2b are the time series of the F10.7 and K_p indexes, which are commonly used to assess the level of solar and geomagnetic activity, for the same time span as the radiated and absorbed power series. Clearly the F10.7 time series most closely mimics the behavior of the absorbed solar power, both in terms of long-term decrease and shorter-term variability. The high frequency variability of the K_p index (visually) mimics the behavior of the infrared time series, but there is no clear visual evidence of a long-term downward decrease in this index. Similar behavior is found in the A_p index (not shown). *Mlynczak et al*. [2007b] noted that the standard deviation of the annual mean NO power was essentially constant despite a decrease in radiated power of nearly a factor of 3. Some process clearly is responsible for maintaining the high-frequency variability of the NO and CO_2 emitted power. The variability in the A_p and K_p indexes is suggestive of continuous, prompt coupling between the infrared energy budget and the geomagnetic environment, previously seen in major geomagnetic storm events [*Mlynczak et al*., 2003; 2005]

Following *Mlynczak et al*. [2007b] we compute the LNP for the time series presented above. Presented in Figures 3, 4, and 5 are the LNP for the NO, CO_2, and the K_p indexes.

Indicated in all figures are the 95% and 50% significance levels. The LNP for both infrared series exhibit a large 60-day peak corresponding to the yaw period of the TIMED spacecraft. The LNP for the NO time series exhibits a series of peaks near 450, 300, and 200 days that exceed the 95% confidence limit. There are also significant peaks at 34.5 days and at 9 days. In addition a number of small peaks occur in the LNP with periods ranging from 2 to 30 days, including peaks at 13.5 and 6.75 days. We note the 13.5, 9, and 6.75 day periods correspond to exact fractions of the 27-day solar rotation period.

The LNP for the CO_2 time series exhibits peaks at 360, 180, and 90 days that correspond to annual, semi-annual, and seasonal variability. The LNP for CO_2 also exhibits a peak at 9 days that is just below the 50% significance level. A smaller peak at 27 days is also evident. We suggest that the strength of the 9-day periodicity may be influenced to some extent by the approach used in the generation of the SABER infrared cooling rates. Specifically, the CO_2 abundance is measured directly by SABER in the daytime (from CO_2 emission at 4.3 μm) but at night a seasonal climatology of CO_2 is used as the 4.3 μm signal essentially vanishes at night due to the absence of solar excitation. This will influence the retrieval of temperature and cooling rates and may thereby suppress the 9-day periodicity. Nevertheless, the cooling rates and computed power are always consistent with the measured radiances at 15 μm. Subsequent versions of the SABER data set will improve the retrieval of CO_2 at night and the influence of the nighttime CO_2 abundance will be examined then in more detail. The strength of the 9-day feature in CO_2 may also be smaller due to the fact that it originates in a lower and denser region of the thermosphere than the NO emission and may not be as subject to the effects of particle precipitation.

The LNP for the absorbed solar power and the F10.7 index (not shown) are similar to each other. Significant periodic features in the absorbed solar power occur near 27 days, 150 days, and 300 days. The LNP for the F10.7 index has peaks at 27, 150, 200 and 300 days, all exceeding the 95% significance level. The 200 and 300-day peaks are also present in the NO LNP power spectrum. There is no spectral power for periods shorter than ~20 days in the time series of absorbed solar ultraviolet radiation and of the F10.7 index.

The LNP for the K_p index (Figure 5) exhibits almost completely opposite behavior to that for the absorbed solar power and the F10.7 index. The LNP for the K_p index (and the A_p index not shown) exhibit no statistically significant peaks (greater than 50%) longer than the 27-day solar rotation period. The LNP for the these two indexes exhibit peaks of 27, 13.5, 9, 6.7, 5.4, and 3.85 days, which are all exact fractions of the 27-day solar rotation period. The 9-day peak is largest in the LNP of both A_p and K_p. The presence of the 9-day peak in the geomagnetic indexes and in the emitted infrared power implies a strong coupling between the geomagnetic environment and the infrared energy budget of the thermosphere.

Discussion and Summary

The LNP calculations presented above provide compelling evidence for strong, prompt, and continuous coupling of the geomagnetic environment to the thermal structure and chemical composition of the thermosphere, which in turn modulates the strength of the infrared emission and radiative cooling of the thermosphere. Such coupling, previously reported in large geomagnetic storm events [e.g., *Mlynczak et al*., 2003, 2005], now appears to be a fundamental process, providing a continuous and significant influence on the thermospheric energy balance, and hence, thermosphere structure and climate.

The origin of the 9-day periodicities in the geomagnetic indexes and in the infrared energy budget is of considerable interest. We note that 9-day periodicities have been observed in the occurrence of high-speed solar wind events [*Verma and Joshi*, 1994]. Recently, *Temmer et al*. [2007] have shown conclusively that a 9-day periodicity exists in the occurrence of coronal hole features on the Sun in the 1998-2006 timeframe. The 9-day periodicity arises from a "triangular" distribution of coronal holes approximately 120 deg apart in solar longitude. Thus the 27-day solar rotation period brings coronal holes in view of the Earth every 9 days.

The solar coronal holes influence the energy balance in the thermosphere through the modulation of the solar wind and hence the deposition of energetic particles into the thermosphere. These in turn alter the thermal structure and chemical composition of the thermosphere thereby changing the infrared emission intensity. We therefore conclude that the periodic variation of the coronal hole features is modulating the solar wind, influencing the amount of energy deposited into the thermosphere, and is responsible for the observed 9-day periodicity in the infrared emissions. These results strongly suggest a direct coupling between the solar corona and upper atmosphere of the Sun and the energy balance in the upper atmosphere of the Earth.

Finally, the prompt nature of the infrared response raises two questions. First, by what mechanisms are the NO and CO_2 emissions driven so rapidly? Second, what is the anticipated response of the radiative cooling by atomic oxygen (O) at 63 μm that is also important in the thermosphere? As discussed previously [*Mlynczak et al*., 2005] the primary mechanisms by which the infrared emission can be altered are changes in temperature, changes in abundance of NO and CO_2, and changes in the atomic oxygen concentration that drives the NO and CO_2 emissions through collisional energy transfer. The NO 5.3-μm emission is 2.8 times more

sensitive to temperature changes than CO_2 15-μm emission and 11.8 times more sensitive to temperature than O 63-μm emission. The NO abundance is also quite variable and can increase greatly during geomagnetic events. In contrast, it is unlikely that the abundance of CO_2 would increase during a geomagnetic event, as there is no ready source of carbon in the thermosphere. Atomic oxygen can increase if there is destruction of molecular oxygen during an event. Thus we speculate that the NO emission changes are due to a combination of temperature, composition, and atomic oxygen changes while CO_2 emission changes are primarily due to changes in temperature and atomic oxygen. The atomic oxygen emission 63 μm is substantially less sensitive to temperature and thus would require changes in its abundance to markedly change its emission rate.

The SABER data offer the first global, long-term look at the radiative cooling of the thermosphere. The data provide fundamental information on the natural variability of the atmosphere on time scales from days to years. Future research with these data will focus on the ability of thermospheric general circulation models to replicate the observed variability. This is a necessary first step to achieving improved quantitative predictions of the effects of anthropogenic increases of carbon dioxide on the thermosphere. In addition we must also investigate in detail the latitudinal variations of the periodic features, again on short and long timescales. It might be expected, for example, that the periodic features would be strongest nearest the geomagnetic poles where the particle precipitation is the greatest. Parameterizations of the infrared emissions and their variations in terms of F10.7, A_p, and K_p should also be developed.

References

Mertens C. J., et al. (2004), SABER observations of mesospheric temperatures and comparisons with falling sphere measurements taken during the 2002 summer MaCWAVE campaign, *Geophys. Res. Lett*., 31, L03105, doi:10.1029/2003GL018605.

Mlynczak, M. G., et al., (2007b), Evidence for a solar cycle influence on the infrared energy budget and radiative cooling of the thermosphere, *J. Geophys. Res*., 112, A12302, doi:10.1029/2006JA012194.

Mlynczak M. G., F. J. Martin-Torres, J. M. Russell III (2007a), Correction to "Energy transport in the thermosphere during the solar storms of April 2002", *J. Geophys. Res*., 112, A02303, doi:10.1029/2006JA012008.

Mlynczak M. G., et al., (2005), Energy transport in the thermosphere during the solar storms of April 2002, *J. Geophys. Res*., 110, A12S25, doi:10.1029/2005JA011141.

Mlynczak M. G., et al., (2003), The natural thermostat of nitric oxide emission at 5.3 μm in the thermosphere observed during the solar storms of April 2002, *Geophys. Res. Lett*., 30 (21), 2100, doi:10.1029/2003GL017693.

Mlynczak, M. G., C. J. Mertens, R. R. Garcia, R. W. Portmann, (1999), A detailed evaluation of the stratospheric heat budget 2. Global radiation balance and diabatic circulations, *J. Geophys. Res*., 104(D6), 6039, doi: 10.1029/1998JD200099.

Mlynczak, M. G., Energetics of the mesosphere and lower thermosphere and the SABER experiment, *Adv. Space Res*., 20, No. 6, 1177-1183, 1997.

Mlynczak, M. G., Energetics of the middle atmosphere: Theory and observation requirements, *Adv. Space Res*., 17, No. 11, 117-126, 1996.

Roble, R. G. and R. E. Dickinson (1989), How will changes in carbon dioxide and methane modify the mean structure of the mesosphere and thermosphere?, *Geophys. Res. Lett*. 16, 1441.

Temmer, M., B. Vrsnak, A. M. Veronig, 2007, Periodic appearance of coronal holes and the related variation of solar wind parameters, *Solar Phys*., 241, 371, doi: 10.1007/s11207-007-0336-1.

Verma, V. K., and G. C. Joshi, On the occurrence rate of high-speed solar wind events, *Solar Phys*., 155, 401-404, 1994.

Woods T. N., et al., Solar EUV Experiment (SEE): Mission overview and first results, *J. Geophys. Res*., 110, A01312, doi:10.1029/2004JA010765, 2005.

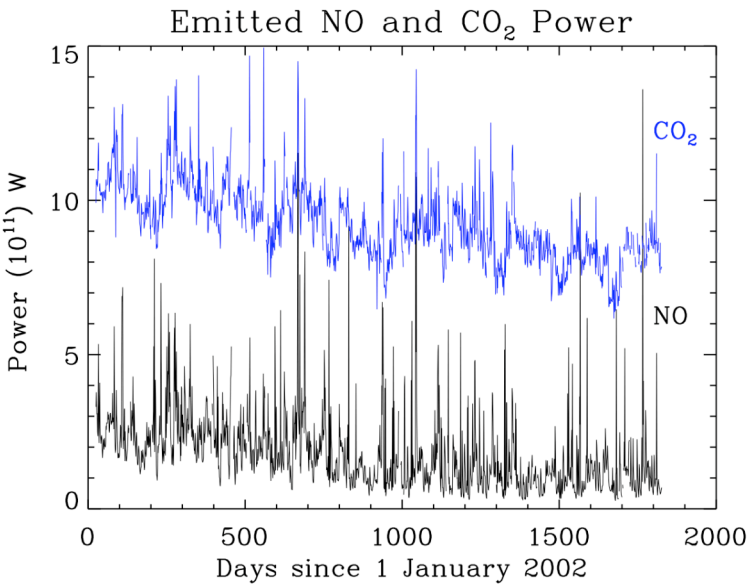

Figure 1a. Time series of daily global radiated power from the thermosphere (100-200 km) from NO and CO_2 from January 2002 through December 2006.

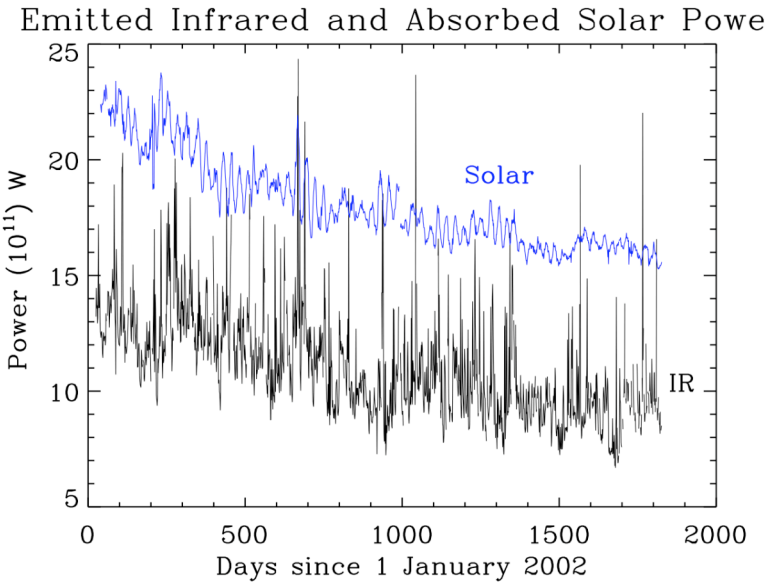

Figure 1b. Time series of daily global absorbed solar power (0 to 175 nm) and radiated infrared (IR) power (CO_2 plus NO) in the thermosphere from January 2002 through December 2006.

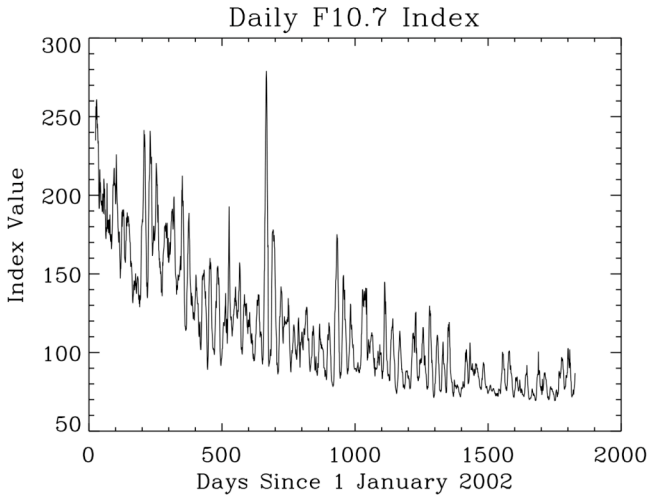

Figure 2a. Time series of daily average F10.7 index from January 2002 through December 2006.

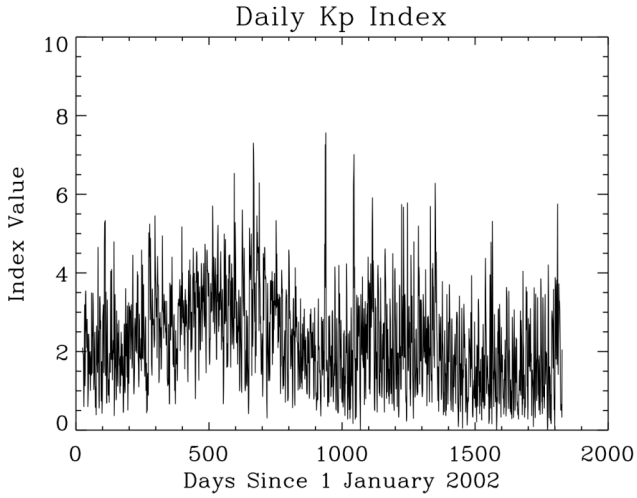

Figure 2b. Time series of daily average K_p index from January 2002 through December 2006.

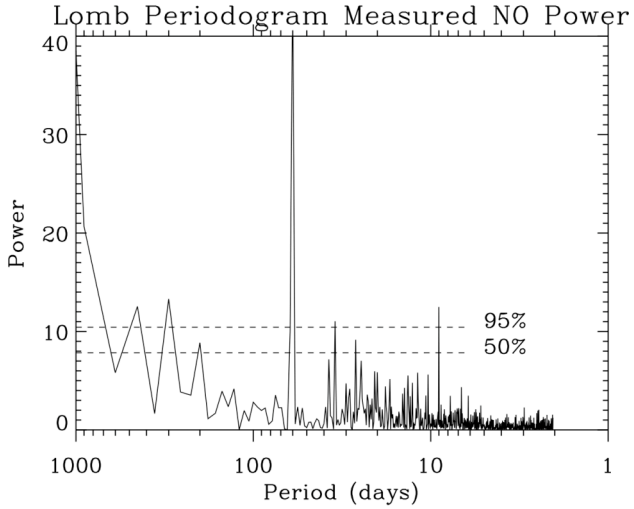

Figure 3. Lomb normalized periodogram of the NO power time series shown in Figure 1a.

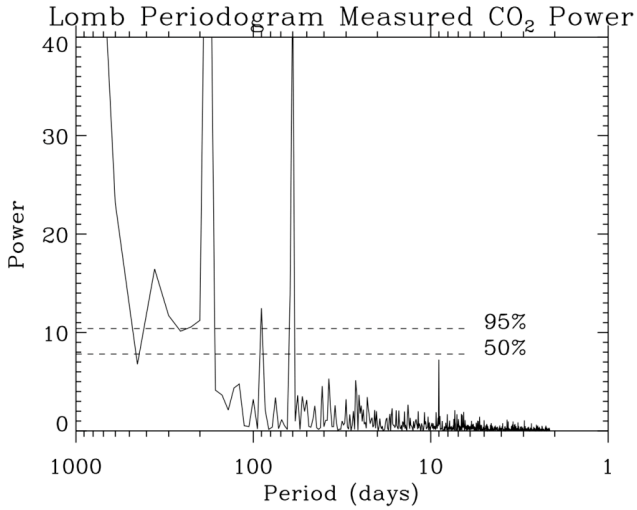

Figure 4. Lomb normalized periodogram of the CO_2 power time series shown in Figure 1b.

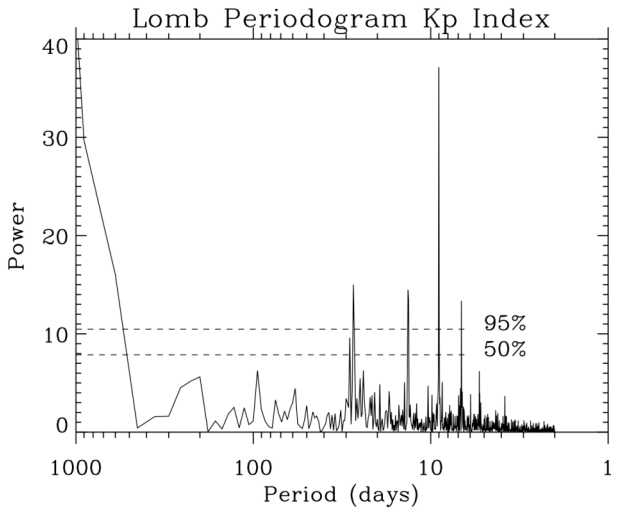

Figure 5. Lomb normalized periodogram of the daily average K_p index time series.